Materials Letters 331 (2023) 133504

Contents lists available at ScienceDirect

Materials Letters

journal homepage: www.elsevier.com/locate/matlet

Wear resistant $CoCrFeMnNi_{0.8}V$ high entropy alloy with multi length-scale hierarchical microstructure

S. González [a,*], A.K. Sfikas [a], S. Kamnis [b], C.G. Garay-Reyes [c], A. Hurtado-Macias [c], R. Martínez-Sánchez [c]

[a] Faculty of Engineering and Environment, Northumbria University, Newcastle upon Tyne NE1 8ST, UK
[b] Castolin Eutectic-Monitor Coatings Ltd, Newcastle upon Tyne NE29 8SE, UK
[c] Centro de Investigación en Materiales Avanzados (CIMAV), Laboratorio Nacional de Nanotecnología, Miguel de Cervantes 120, 31136 Chihuahua, Chih., Mexico

ARTICLE INFO

Keywords:
Metal and alloys
Indentation and hardness
Wear and tribology
Solidification

ABSTRACT

This work shows a $CoCrFeMnNi_{0.8}V$ high entropy alloy (HEA) with multiple length-scale hierarchical microstructure, obtained upon cooling at ~62.5 K/s, consisting of a dominant globular sigma phase, FCC matrix and V-rich particles. The novel microstructure, never reported before for the CoCrFeMnNiV system, results in about a fourfold and sixfold increase of hardness and wear resistance, respectively, compared to that of CoCrFeMnNi alloy.

1. Introduction

The most well known among all FCC-type high entropy alloys (HEAs) is the CrMnFeCoNi (Cantor alloy) [1,2]. The addition of Cr and Mn destabilise single phase solid solution and promotes the formation of σ phase while Ni is a strong FCC stabiliser and supresses the formation of σ phase [3]. The effect of Ni on $CoCrFeMnNi_xV$ alloy is similar since it reduces the volumen fraction of σ phase and therefore decreases the microhardness from 12 GPa for CoCrFeMnV to 4.1 GPa for $CoCrFeMnNi_3V$ [4]. However, the microstructure of the novel composition $CoCrFeMnNi_{0.8}V$ produced upon casting at a cooling rate of ~62.5 K/s and its influence on the hardness and wear resistance have not been studied before.

2. Experimental procedure

The master alloys were fabricated from elements with purity higher than 99.9 at.%. Subsequently they were re-melted at least three times using a Zr-getter in a high purity argon atmosphere. Rod samples of 8 mm diameter were obtained by melting the master alloy into a water-cooled copper mould in an inert gas atmosphere. X-ray diffraction (XRD) was used to analyse the structure. A Scanning Electron Microscope (SEM) and Transmission Electron Microscope (TEM) with energy-dispersive X-ray (EDX) analysis were used to analyse the microstructures. Nanoindentation experiments were performed at room temperature in a UMIS equipment from Fischer-Cripps Laboratories, in the load control mode and using a Berkovich-type diamond tip. The surfaces were mirror-like polished prior to the tests. From the 9 nanoindentations performed and the high load applied (2 mN) we have sampled all the existing phases and obtained a statistical mean value. The nanoindentation equipment was used in scratch mode for the scratch tests of the mirror-like polished samples. The 50 μm length scratches were performed at a load of 1.5 mN at a stage speed of 20 μm/s.

3. Results and discussion

The cooling rate $\dot{T}$ of the CoCrFeMnNi and $CoCrFeMnNi_{0.8}V$ suction cast alloys can be estimated from the relationship [5]:

$$\dot{T}\left(\frac{K}{s}\right) = \frac{10}{R^2}\left(\frac{1}{cm^2}\right) \quad (1)$$

where R (4 mm) is the sample radius; hence the cooling rate is ~62.5 K/s for both compositions. Fig. 1 shows the X-ray diffactograms, back-scattered SEM images and compositional mappings for of the alloys. For CoCrFeMnNi, the XRD peaks are associated to a single FCC phase while for $CoCrFeMnNi_{0.8}V$ the XRD peaks correspond to body centred tretragonal σ phase (most abundant) and FCC phase.

For CoCrFeMnNi HEA (Fig. 1a), the microstructure is basically

* Corresponding author.
E-mail address: Sergio.sanchez@northumbria.ac.uk (S. González).

https://doi.org/10.1016/j.matlet.2022.133504
Received 28 October 2022; Received in revised form 8 November 2022; Accepted 9 November 2022
Available online 14 November 2022

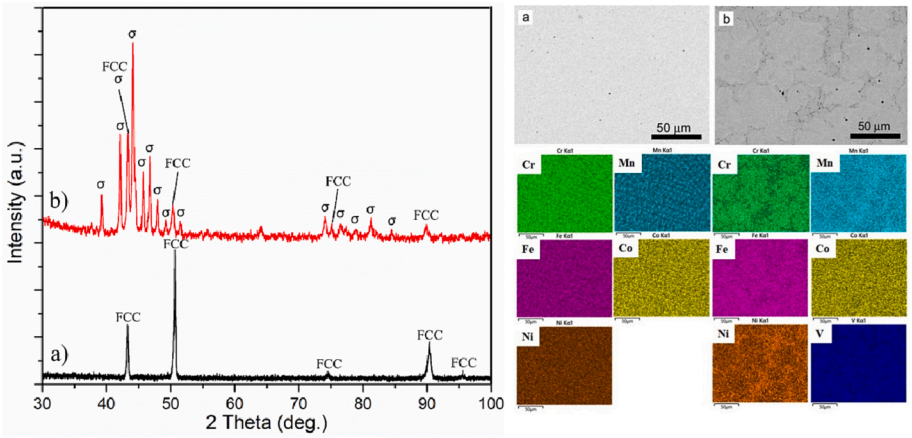

Fig. 1. X-ray diffractograms for a) CoCrFeMnNi and b) $CoCrFeMnNi_{0.8}V$ and backscattered SEM images with compositional mappings for: a) CoCrFeMnNi and b) $CoCrFeMnNi_{0.8}V$.

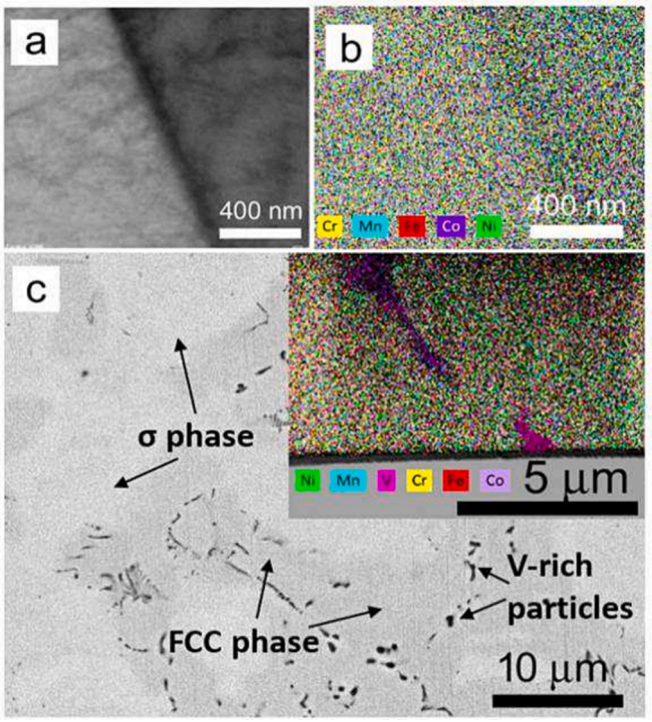

Fig. 2. a) Tem image for CoCrFeMnNi and b) corresponding elemental mapping. c) Backscattered SEM image for $CoCrFeMnNi_{0.8}V$ and inset showing elemental TEM mapping of the V-rich particles.

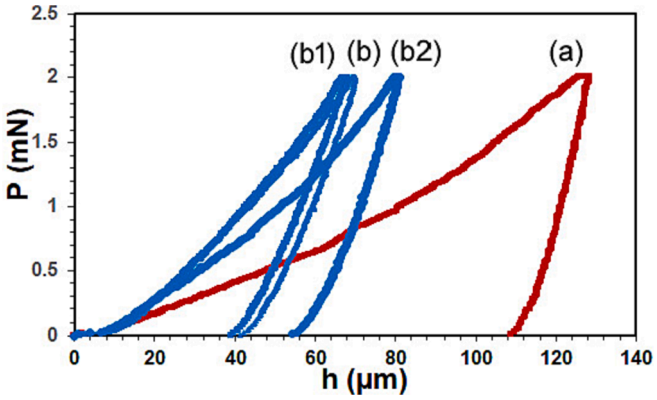

Fig. 3. Load-displacement (P-h) nanoindentation curves for (a) CoCrFeMnNi, (b) $CoCrFeMnNi_{0.8}V$, (b1) σ phase and (b2) matrix.

featurless. However, for $CoCrFeMnNi_{0.8}V$ (Fig. 1b) it consists of dendrites of clear tonality surrounded by a matrix containing tiny dark particles mostly decorating the borders of the dendrites, something intimately connected with the so-called complete and incomplete wetting of grain boundaries by the liquid or second solid phase [6,7]. The presence of the tiny dark particles (lenticular precipitates) seem to precipitate with non-zero contact angle thus suggesting incomplete (partial) wetting. The compositional mappings suggest the CoCrFeMnNi alloy is chemically homogeneous. However, for $CoCrFeMnNi_{0.8}V$, a Cr-rich globular phase surrounded by a Ni-rich matrix is detected, while the distribution of Mn, V, Fe and Co is constant throughout both regions. The Cr-rich phase corresponds to the σ phase, while the Ni-rich phase is associated to the FCC solid solution. The TEM image for CoCrFeMnNi (Fig. 2a) and corresponding compositional mapping (Fig. 2b) shows an homogeneous distribution of the elements throughout the sample, without any sign of segregation to the grain boundaries, thus confirming the previous results (Fig. 1). For the $CoCrFeMnNi_{0.8}V$ HEA, the backscattered SEM image of Fig. 2c shows dark particles of about 1 μm size that according to the TEM mapping (see inset of Fig. 2c), they are very rich in V element and contains cobalt. From linear intercept analysis, the volume fraction of the different phases are: σ phase (~82 vol%), FCC phase (~13 vol%) and V-rich particles (<5 vol%). These particles are finely and homogeneously distributed across the sample and therefore are not the result of unmelted element. To the author's knowledge, this is the first time that such a hierarchical microstructure containing V-rich particles is detected, not present even for similar compositions such as CoCrFeMnNiV HEA [4].

The formation of these V-rich particles seems to be mostly promoted by the relatively low Ni content and therefore the higher probability of the V atoms to be surrounded by the Co, Cr, Fe and Mn atoms while the small particle size and heterogeneous distribution would be favoured by the high cooling rate. From a thermodynamic point of view, the V-Co pairs are more likely to be formed taking into consideration the heats of mixing (V-Co: −14 KJ/mol, V-Ni: −18 KJ/mol, V-Cr: −2 KJ/mol; V-Fe: −7 KJ/mol and V-Mn: −1 KJ/mol [8]). Fig. 3 shows the representative load–displacement (P-h) curves when testing (a) CoCrFeMnNi, (b) $CoCrFeMnNi_{0.8}V$ and also each individual phase: (b1) σ phase and (b2) matrix (FCC + V-rich particles). The maximum indentation depth, also called displacement depth, h_{max}, decreases from 129.9 μm for CoCrFeMnNi to 70.8 μm for $CoCrFeMnNi_{0.8}V$, probably due to the large volume fraction of hard σ phase and V-rich particles. To better understand the contribution of the σ phase and matrix (FCC + V-rich particles)

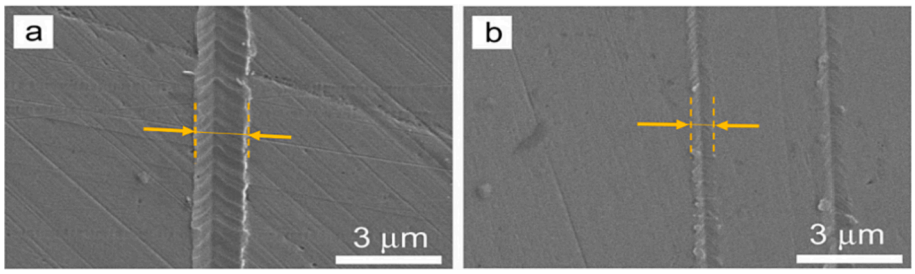

Fig. 4. SEM Images showing the scratches on the samples (a) for CoCrFeMnNi and (b) $CoCrFeMnNi_{0.8}V$ HEAs.

on the overall mechanical behaviour they have been indented individually (Fig. 3).

The wear resistance can be estimated from the H/E_r ratio [9]. This parameter can therefore be used to estimate the wear resistance of each individual phase. For σ phase the H/E_r ratio is 0.057 while for the matrix (FCC + V-rich particles) it is 0.039, therefore most of the wear resistance contribution is attributed to the σ phase (~82 vol%). The relatively small h_{max} value for the $CoCrFeMnNi_{0.8}V$ is consistent with the hardness since it is higher for $CoCrFeMnNi_{0.8}V$, i.e., 13.09 GPa than for CoCrFeMnNi, i.e., 3.80 GPa. The H/E_r ratio is higher for $CoCrFeMnNi_{0.8}V$ (i.e., 0.049) than for CoCrFeMnNi (i.e., 0.018), a threefold wear resistance increase. The wear resistance has been also studied directly from nanoscratch tests on CoCrFeMnNi (Fig. 4a) and $CoCrFeMnNi_{0.8}V$ (Fig. 4b) by performing 50 μm long nanoscratches, long enough to embrace all the phases.

The scratch width for CoCrFeMnNi is 1.5 μm, while for $CoCrFeMnNi_{0.8}V$ (see yellow arrows in Fig. 4a and b, respectively) it is only 0.6 μm. A useful parameter to study the wear resistance of materials is the scratch hardness number, which is given by the following equation [10]:

$$H_s = q\frac{4 * P}{\pi * \omega'^2} \quad (2)$$

where P (N) the normal load, w' (m) the scratch width and H_S (Pa) is the scratch hardness. For these alloys, the response can be approximated to a rigid plastic and therefore q = 2, which is also used in metallic composites [11]. From equation I, the scratch hardness of CoCrFeMnNi equals 1.70 GPa while for $CoCrFeMnNi_{0.8}V$ it is 10.61 GPa, much higher than for Stellite® 6 (4.3 GPa) and for $FeCoCrNiW_{0.3}$ (1.25 GPa), $FeCoCrNiW_{0.3}$ + 5 a. % C (4.5 GPa) [12]. No cracks have been detected around the scratches and no pop-ins associated to the formation of cracks are detected (Fig. 3), thus suggesting the $CoCrFeMnNi_{0.8}V$ HEA is more ductile than other alloys such as metallic glass composites [13]. Another important parameter that can be obtained from the scratch tests are the pile-up height and total groove depth, which are indicative of how ductile or brittle a material is. The groove height for CoCrFeMnNi and $CoCrFeMnNi_{0.8}V$ are 134 and 26 nm, respectively, while the pile-up height is 32 nm and 21 nm respectively, which is consistent with the higher wear resistance of $CoCrFeMnNi_{0.8}V$ alloy.

This work demonstrates that the microstructure of the CoCrFeMnNiV alloy system is very sensitive to small changes in composition and cooling rate, which enables to easily tweak their performance for their practical application in industry. For example, the hardness of the novel $CoCrFeMnNi_{0.8}V$ is higher than for CoCrFeMnV, while the opposite should be expected [4]. This could be attributed to the hierarchical microstructure containing V-rich particles when cooling at ~62.5 K/s.

4. Conclusions

The following conclusions can be drawn:

1. A novel $CoCrFeMnNi_{0.8}V$ high entropy alloy (HEA) with multi length-scale hierarchical microstructure consisting of sigma phase (~82 vol%), FCC phase (~13 vol%) and V-rich particles containing Co (<5 vol%) is obtained directly upon suction casting at a cooling rate of ~62.5 K/s.
2. The hardness for $CoCrFeMnNi_{0.8}V$, 13.09 GPa, is nearly 4 times higher than for CoCrFeMnNi while the scratch hardness number, a measure of the wear resistance, is 10.61 GPa, about 6 times higher than for CoCrFeMnNi.
3. The presence of V-rich particles is detected for the first time in the CoCrFeMnNiV alloy system.
4. This work demonstrates that combined small changes of composition and cooling rate can lead to a $CoCrFeMnNi_{0.8}V$ alloy of potential interest for durable components.

CRediT authorship contribution statement

S. González: Conceptualization, Writing – original draft, Supervision, Investigation. **A.K. Sfikas:** Writing – original draft, Investigation. **S. Kamnis:** Investigation, Funding acquisition. **C.G. Garay-Reyes:** Investigation, Formal analysis. **A. Hurtado-Macias:** Writing – original draft, Investigation. **R. Martínez-Sánchez:** Investigation, Formal analysis.

Declaration of Competing Interest

The authors declare the following financial interests/personal relationships which may be considered as potential competing interests: Spyros Kamnis reports financial support was provided by UK Research and Innovation. NA reports a relationship with NA that includes:. NA has patent NA pending to NA. No conflict of interests.

Data availability

Data will be made available on request.

Acknowledgements

The authors would like to acknowledge the support from the UK Research & Innovation (UKRI-IUK) national funding agency. Project Grant: 53662 '*Design of High-Entropy Superalloys Using a Hybrid Experimental-Based Machine Learning Approach: Steel Sector Application*'. The authors are deeply grateful to Roberto P. Talamantes Soto for his valuable support with scratch tests.

References

[1] B. Cantor, I.T.H. Chang, P. Knight, A.J.B. Vincent, Mater. Sci. Eng. A 375–377 (2004) 213–218.
[2] J.W. Yeh, S.K. Chen, S.J. Lin, J.Y. Gan, T.S. Chin, T.T. Shun, C.H. Tsau, S.Y. Chang, Adv. Eng. Mater. 6 (2004) 299–303.
[3] K.A. Christofidou, T.P. McAuliffe, P.M. Mignanelli, H.J. Stone, N.G. Jones, J. Alloys Compd. 770 (2019) 285–293.
[4] M.V. Karpets', O.M. Myslyvchenko, O.S. Makarenko, J. Superhard. Mater. 37 (2015) 182–188.
[5] X. Lin, W. Johnson, J. Appl. Phys. 78 (1995) 6514.
[6] B.B. Straumal, A. Korneva, A. Kuzmin, G.A. Lopez, E. Rabkin, A.B. Straumal, G. Gerstein, A.S. Gornakova, Metals 11 (2021) 1881.

[7] B.B. Straumal, A. Korneva, G.A. Lopez, A. Kuzmin, E. Rabkin, G. Gerstein, A. B. Straumal, A.S. Gornakova, Materials 14 (2021) 7506.
[8] F.R. Boer, D.G. Perrifor, Cohesion in Metals, Elsevier Science Publishers B.V, Netherlands, 1988.
[9] A. Leyland, A. Matthews, Wear 246 (2000) 1–11.
[10] M. Villapún, F. Esat, S. Bull, L.G. Dover, S. González, Materials 10 (2017) 506.
[11] S.K. Sinha, S.U. Reddy, M. Gupta, Tribol. Int. 39 (2006) 184–189.
[12] M.G. Poletti, G. Fiore, F. Gili, D. Mangherini, L. Battezzati, Mater. Design 115 (2017) 247–254.
[13] V.M. Villapún, H. Zhang, C. Howden, L. Cheung Chow, F. Esat, P. Pérez, J. Sort, S. Bull, J. Stach, S. González, Mater. Design 115 (2017) 93–102.